

## Supplementary Information

# Tunable large-scale regular array of topological defects in nematic liquid crystals

**MinSu Kim and Francesca Serra\***

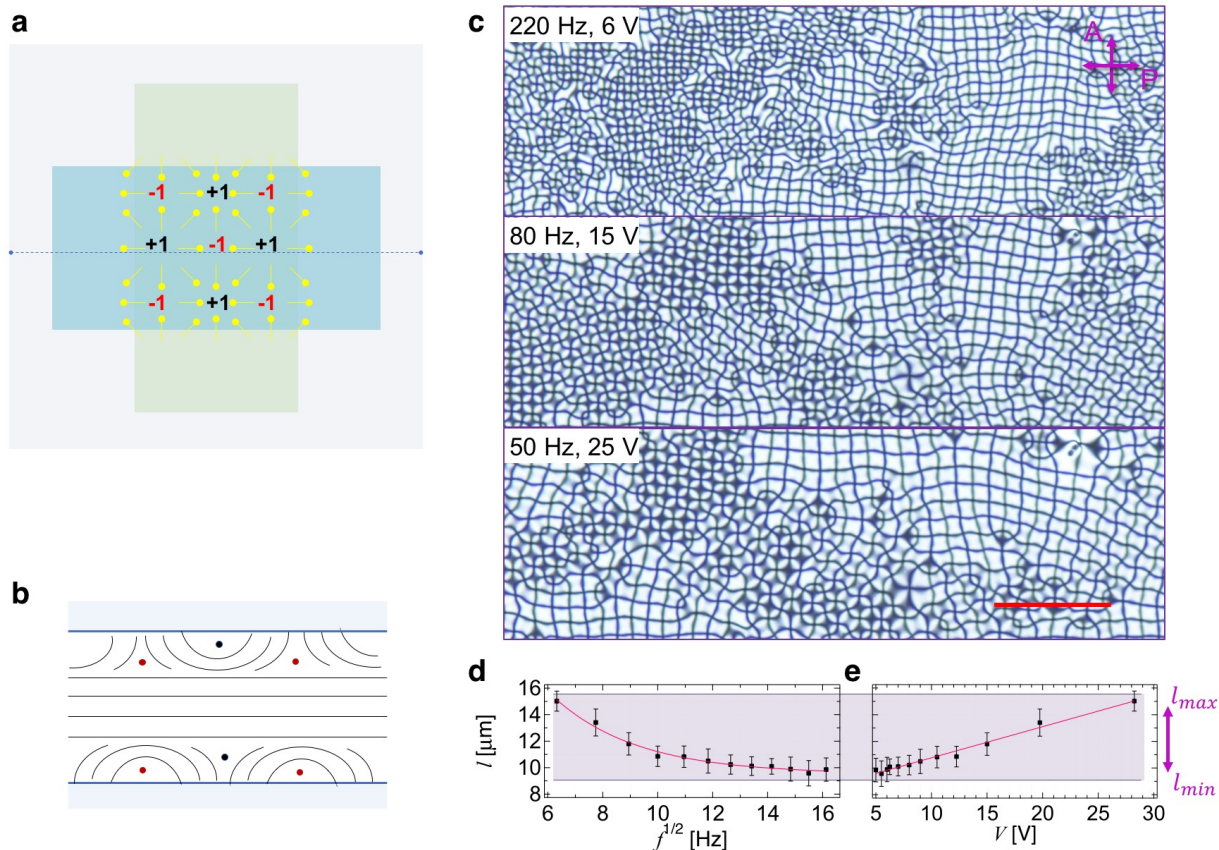
Department of Physics and Astronomy, Johns Hopkins University, Baltimore 21218, USA

\*francesca.serra@jhu.edu

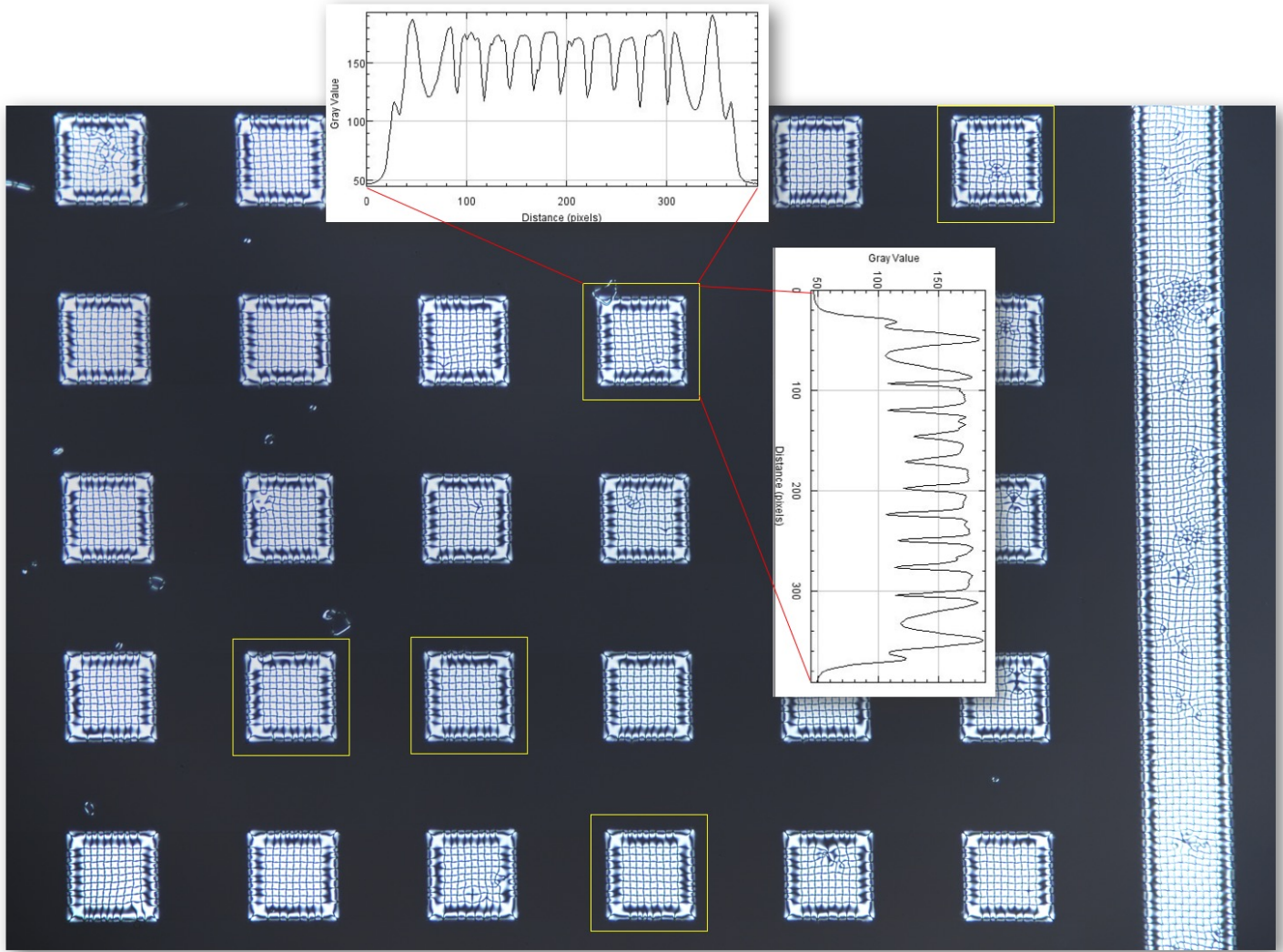
The list in the Supporting Information

1. Supplementary Figures S1-S6.
2. Supplementary Table S1.
3. Supplementary Video captions S1-S7.

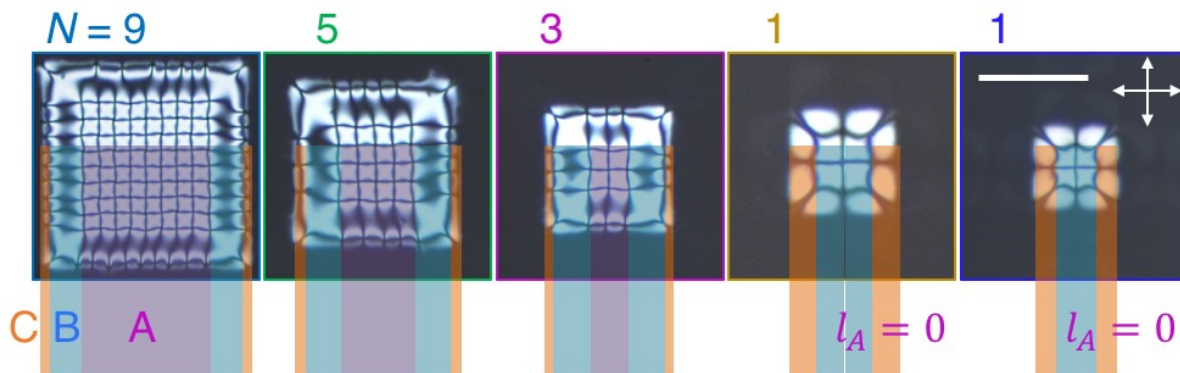
## Supplementary Figures



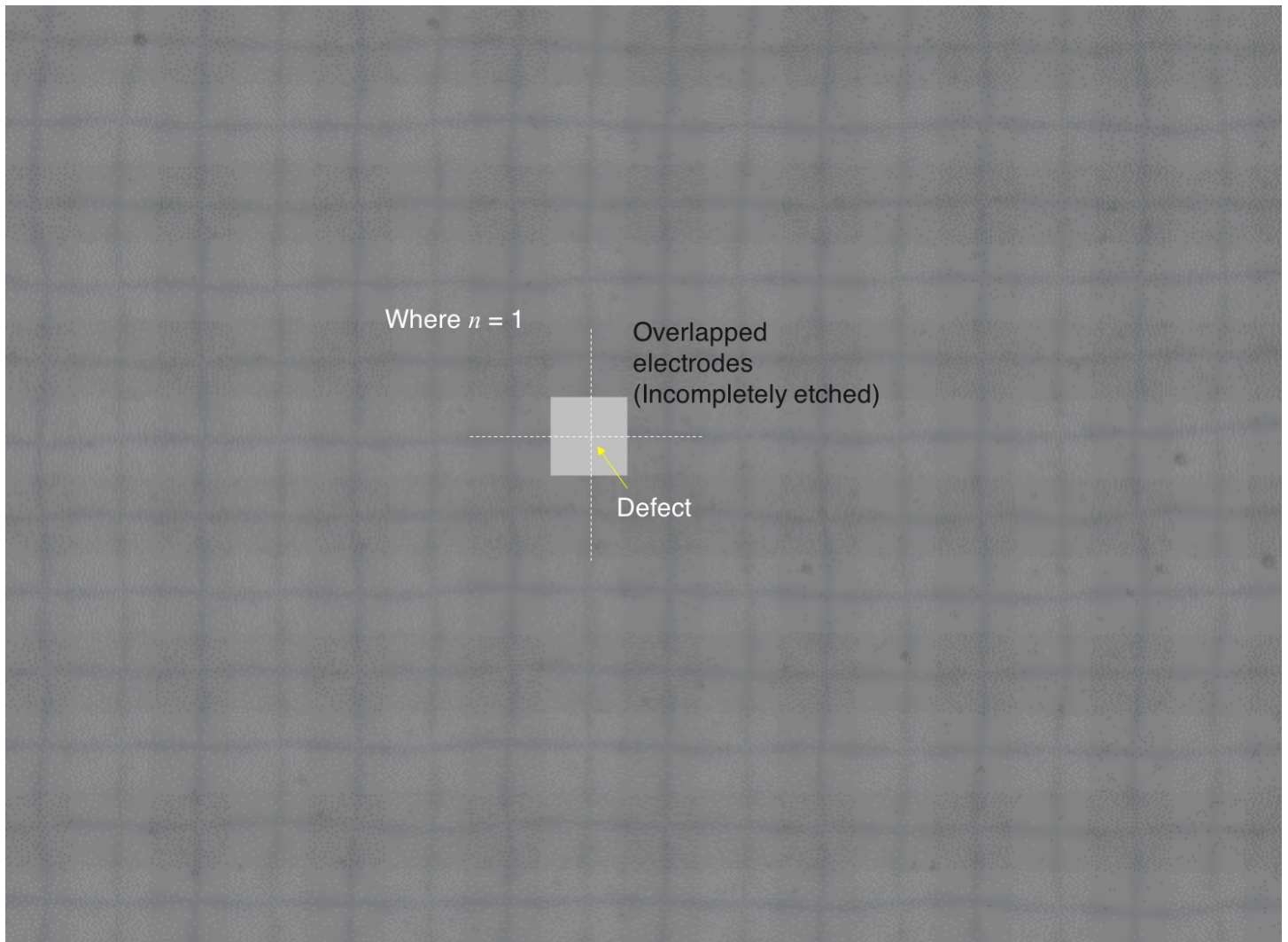
**Supplementary Figure S1.** a,b) Schematic illustration of director fields of umbilical defect arrays a) in the  $x$ - $y$  plane with fully-patterned electrodes and b) in the  $x$ - $z$  plane. c-e) The behavior of the distance between neighboring defects  $l$  as a function of frequency  $f$  and voltage  $V$  in plain electrodes. c) Polarizing optical microscopy (POM) images of irregular defect arrays as a function of  $f$  and  $V$  (see Movie S1 for sequential images, Supporting Information). The purple double-headed arrows represent polarizers. The scale bar is 100  $\mu\text{m}$ . d,e) Measured  $l$  as a function of  $f^{1/2}$  and  $V$ , which is in a range of  $l_{\text{min}} \sim 9.5 \mu\text{m}$  and  $l_{\text{max}} \sim 15 \mu\text{m}$  with a liquid crystal layer thickness  $d \sim 3.7 \mu\text{m}$ .



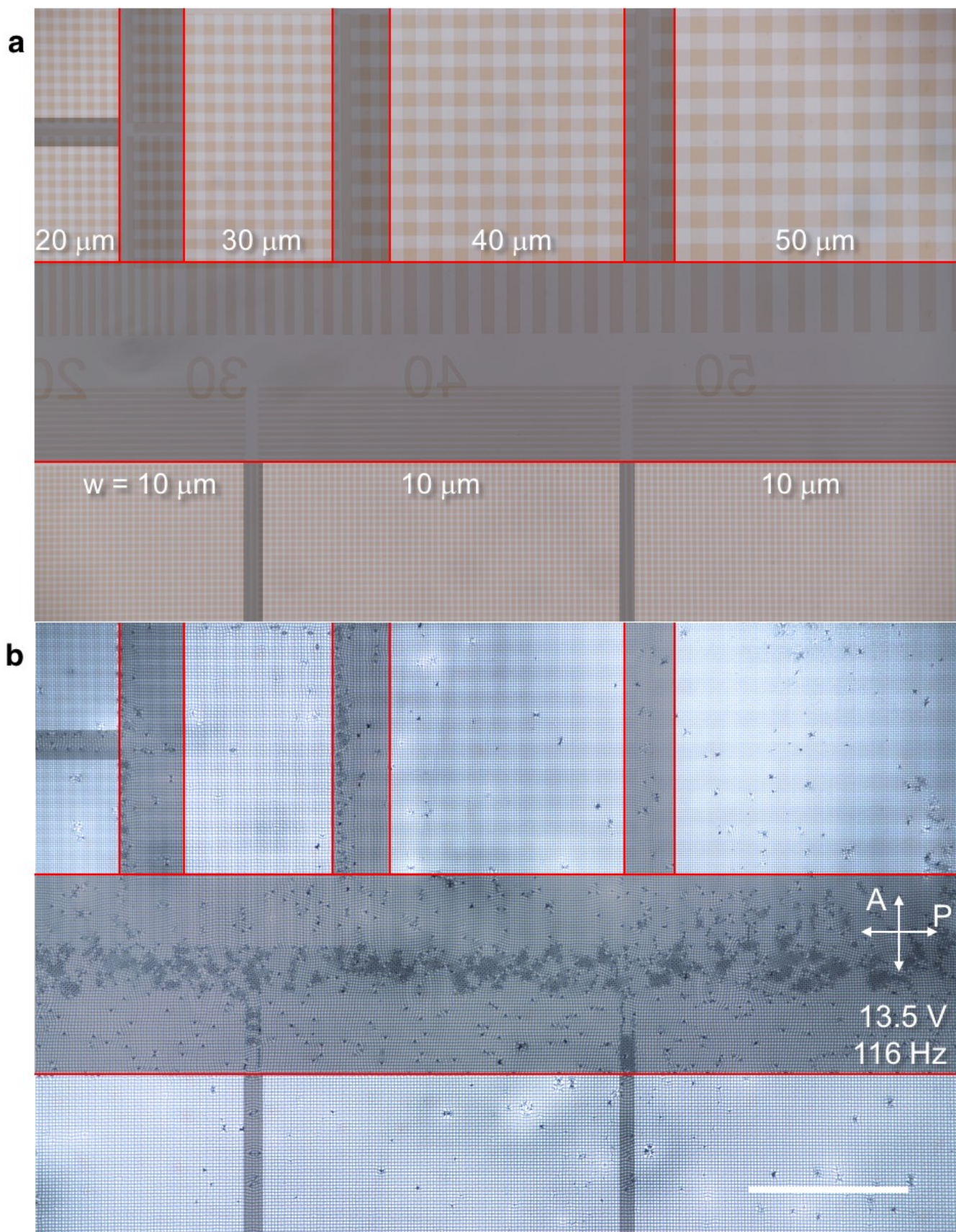
**Supplementary Figure S2.** Quantification of characteristic spacing and defect arrays. We chose 5 regions of interest (ROI) in each set of measurement for field-active areas to measure the characteristic spacing and other physical quantities by using an image processing software (ImageJ).<sup>1</sup>



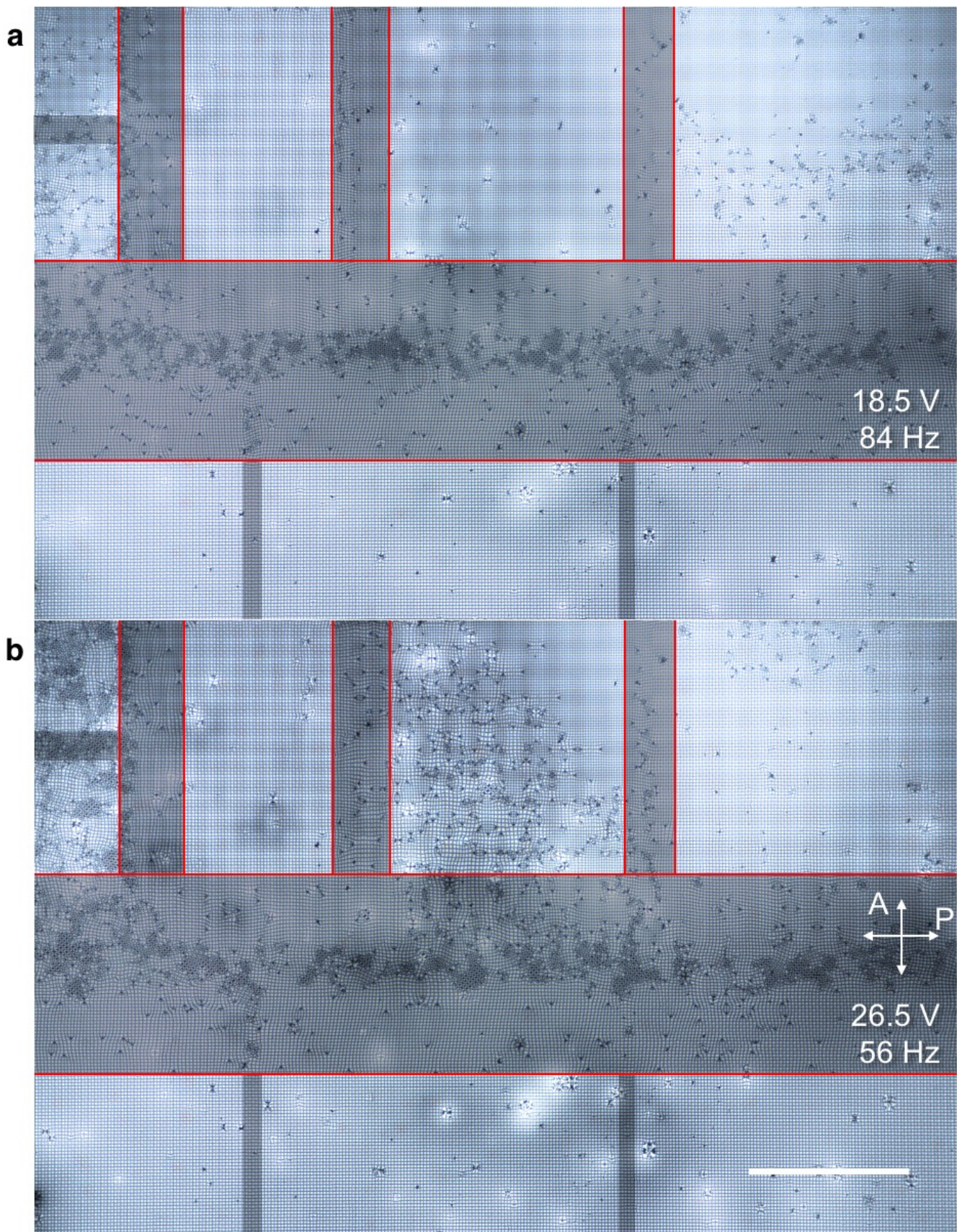
**Supplementary Figure S3.** The field-edge effect at the area under lateral electric fields. The regular array area (region A), edge region between the zeroth and the first dark lines (region B) and the outermost region (region C). The length of region A,  $l_A = 0$  where  $N = 1$ . The white double-headed arrows represent polarizers. The scale bar is  $50 \mu\text{m}$ .



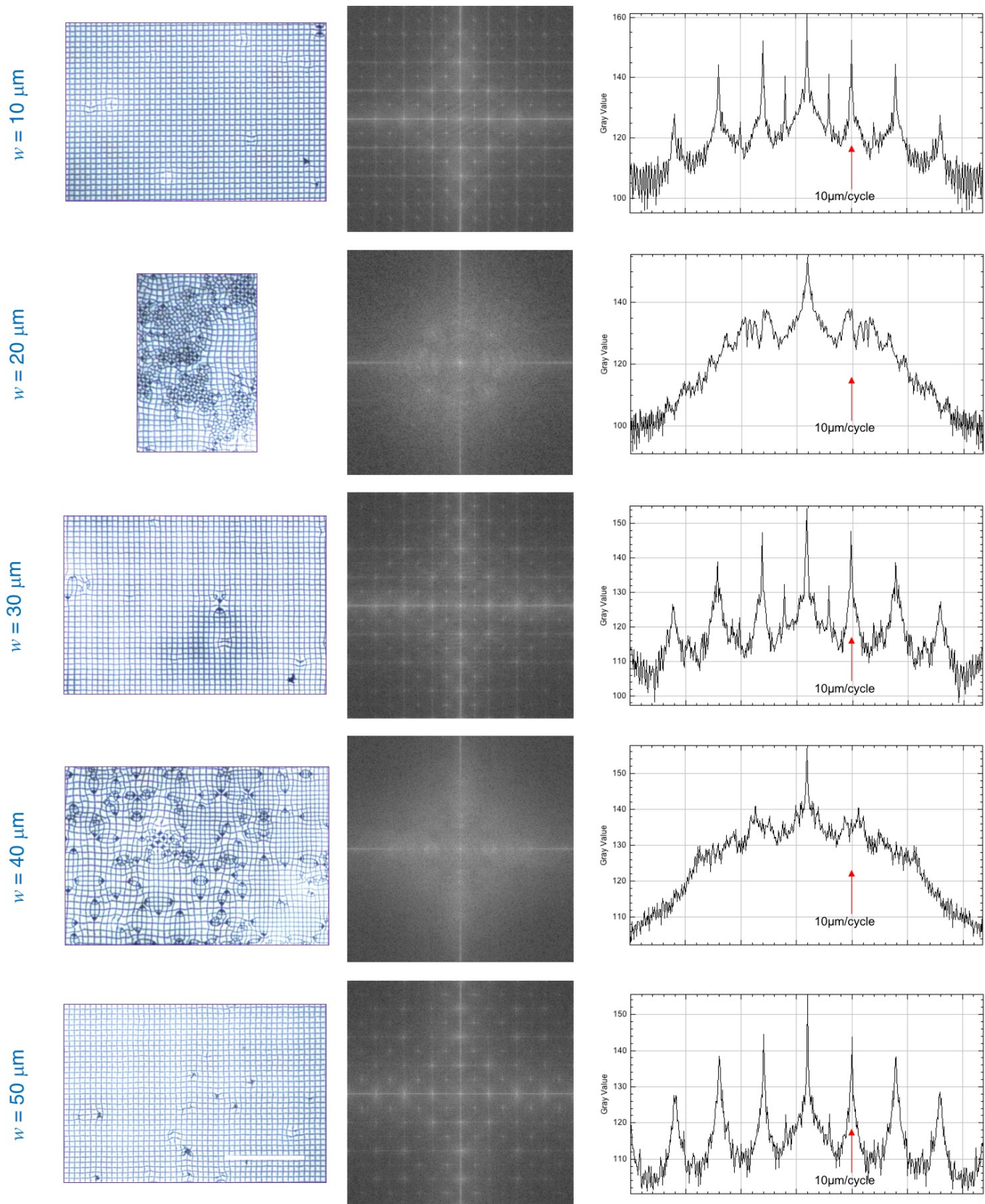
**Supplementary Figure S4.** In large-scale array with incompletely etched electrodes, umbilical defects are produced at the center of the patterns of the overlapped electrodes, where the number of defects  $n = 1$ .



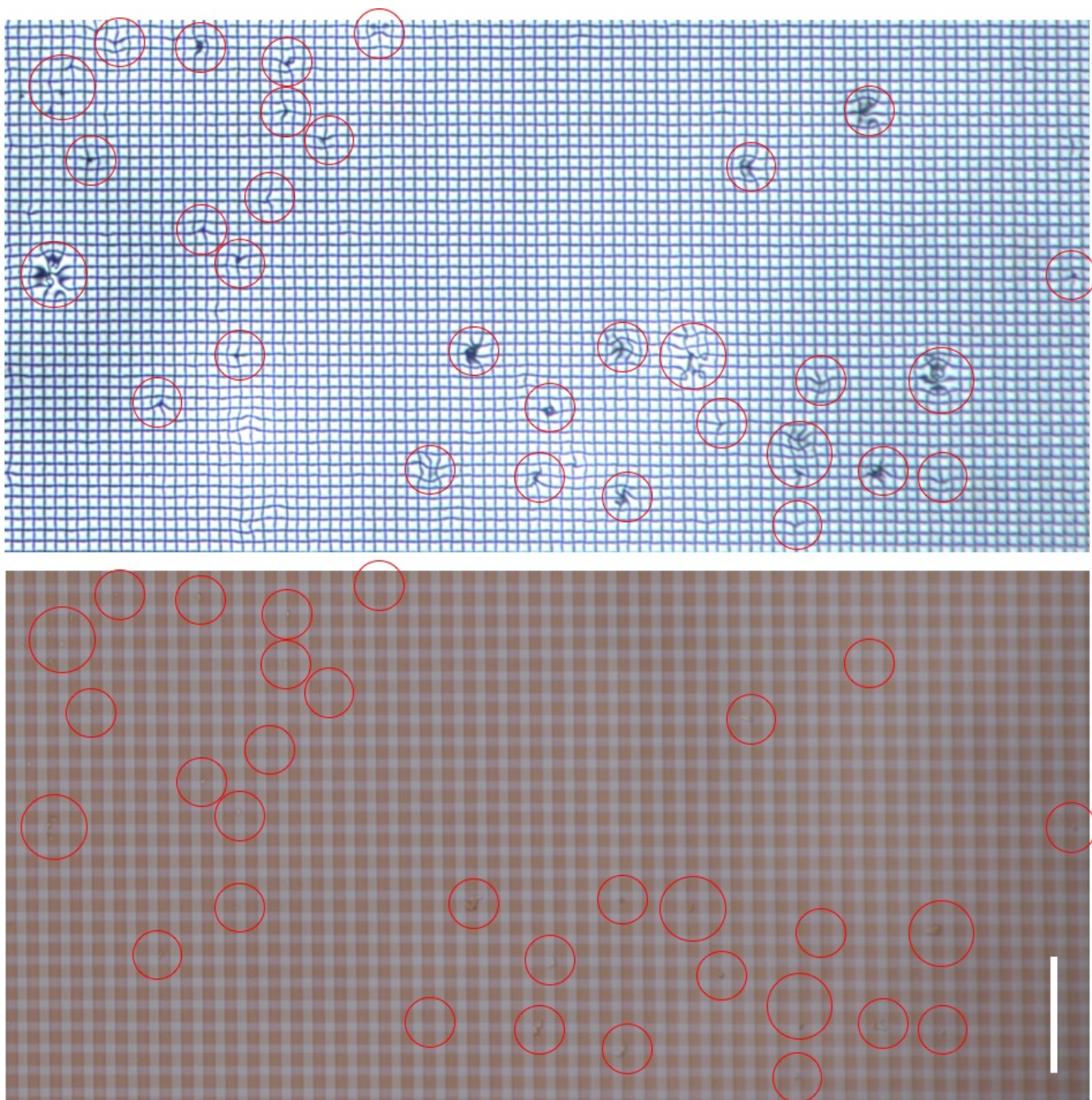
**Supplementary Figure S5.** The size dependence of regular arrays. a) The *incompletely* etched electrodes with the electrode width  $w = 10, 20, 30, 40,$  and  $50 \mu\text{m}$  in the relatively bright regions. The red lines indicate the boundaries. b) The regular arrays appear at  $13.5 \text{ V}$  and  $116 \text{ Hz}$ . The scale bar is  $500 \mu\text{m}$ .



**Supplementary Figure S6.** The size dependence of regular arrays with the incompletely etched electrodes with the width  $w = 10, 20, 30, 40,$  and  $50 \mu\text{m}$  in the relatively bright regions. The red lines indicate the boundaries. a,b) The regular arrays appear at a) 18.5 V and 84 Hz and b) 26.5 V and 56 Hz. The scale bar is 500  $\mu\text{m}$ .



**Supplementary Figure S7.** The 2D and 1D Fast Fourier transform (FFT) values of the arrays corresponding to the third column at 26.5 V, 56 Hz in Fig. 4. The electrode width  $w = 10, 30, 50 \mu\text{m}$  can accommodate  $l_w = 10 \mu\text{m}$  arrays with  $n = 1, 3, 5$  whereas  $w = 20, 40 \mu\text{m}$  shows an intermediate state that contains many dislocations between regular states of arrays. The scale bar is  $100 \mu\text{m}$ .



**Supplementary Figure S8.** The contamination corresponding to the imperfection in a defect array. The red circles indicate the contaminated area applied by a) 26.5 V and 56 Hz. b) The contamination on the surface. (The contrast of the image was sharpened for visibility.) The scale bar is 100  $\mu\text{m}$ .

**Table S1.** The *measured* characteristic spacing  $l_{w,m}$ , the number of defects  $n$ , and the *estimated*  $l_{w,e}$ .

$V^a$ [V]	$f^b$ [Hz]	$l_{w,e}^c$ [ $\mu\text{m}$ ]					$l_{w,m}^d$ [ $\mu\text{m}$ ] $\pm$ std. $^e$ [ $\mu\text{m}$ ] ( $n$ ) $^f$				
		10 $^g$	20	30	40	50	10	20	30	40	50
12.0	132	9.4	7.7	9.4	7.9	7.6	9.9 $\pm$ 0.3 (1)	7 $\pm$ 1 (3)	9.9 $\pm$ 0.6 (3)	7.9 $\pm$ 0.3 (5)	7.2 $\pm$ 0.4 (7)
12.8	124	9.4	7.3	9.4	7.9	7.5	9.9 $\pm$ 0.3 (1)	6.7 $\pm$ 0.4 (3)	9.9 $\pm$ 0.6 (3)	7.9 $\pm$ 0.3 (5)	7.1 $\pm$ 0.3 (7)
13.5	116	9.4	7.4	9.4	7.9	7.5	9.9 $\pm$ 0.3 (1)	6.7 $\pm$ 0.4 (3)	9.9 $\pm$ 0.6 (3)	7.9 $\pm$ 0.4 (5)	7.1 $\pm$ 0.3 (7)
14.3	108	9.4	7.3	9.4	7.9	7.5	9.9 $\pm$ 0.3 (1)	6.7 $\pm$ 0.4 (3)	9.9 $\pm$ 0.6 (3)	7.9 $\pm$ 0.3 (5)	7.1 $\pm$ 0.3 (7)
15.8	100	9.4	8.7	9.4	7.9	8.3	9.9 $\pm$ 0.3 (1)	8 $\pm$ 3 (3)	9.9 $\pm$ 0.5 (3)	7.9 $\pm$ 0.3 (5)	8 $\pm$ 2 (7)
17.0	92	9.4	8.5	9.4	7.9	9.5	9.9 $\pm$ 0.3 (1)	7 $\pm$ 2 (3)	9.9 $\pm$ 0.4 (3)	7.9 $\pm$ 0.3 (5)	10 $\pm$ 5 (5)
18.5	84	9.4	15.1	9.4	7.9	10.2	9.9 $\pm$ 0.3 (1)	13 $\pm$ 10 (2)	9.9 $\pm$ 0.4 (3)	7.9 $\pm$ 0.4 (5)	12 $\pm$ 5 (4)
20.3	76	9.4	30.7	9.4	7.9	9.5	9.9 $\pm$ 0.3 (1)	27 $\pm$ 35 (1)	9.9 $\pm$ 0.4 (3)	7.9 $\pm$ 0.4 (5)	10.0 $\pm$ 0.4 (5)
22.3	68	9.4	14.5	9.4	7.9	9.5	9.9 $\pm$ 0.3 (1)	13 $\pm$ 6 (2)	9.9 $\pm$ 0.4 (3)	7.9 $\pm$ 0.4 (5)	10.0 $\pm$ 0.4 (5)
23.8	64	9.4	10.2	9.4	8.5	9.5	9.9 $\pm$ 0.3 (1)	15 $\pm$ 9 (1)	9.9 $\pm$ 0.4 (3)	8 $\pm$ 2 (5)	10.0 $\pm$ 0.4 (5)
25.0	60	9.4	15.1	9.4	8.0	9.5	9.9 $\pm$ 0.3 (1)	19 $\pm$ 14 (1)	9.9 $\pm$ 0.4 (3)	9 $\pm$ 3 (4)	10.0 $\pm$ 0.4 (5)
26.5	56	9.4	8.4	9.4	10.5	9.5	9.9 $\pm$ 0.3 (1)	14 $\pm$ 4 (1)	9.9 $\pm$ 0.4 (3)	12 $\pm$ 7 (3)	10.0 $\pm$ 0.4 (5)
28.5	52	9.4	15.9	9.4	9.3	9.5	9.9 $\pm$ 0.3 (1)	13 $\pm$ 6 (2)	9.9 $\pm$ 0.4 (3)	10 $\pm$ 3 (4)	10.0 $\pm$ 0.4 (5)
35.3	48	9.4	0.0	9.4	11.7	9.5	9.9 $\pm$ 0.3 (1)	42 $\pm$ 49 (0)	9.9 $\pm$ 0.4 (3)	13 $\pm$ 1 (3)	10.0 $\pm$ 0.4 (5)

$^a$ ) Voltage;  $^b$ ) Frequency;  $^c$ )  $l_{w,e} \sim (r^2 - \beta \cdot \frac{K\pi^2 - \epsilon V^2}{2f\gamma}) \cdot (\frac{n}{w})$ ;  $^d$ ) Characteristic spacing;  $^e$ ) Standard deviation of  $l_{w,m}$ ;  $^f$ ) The number of defects;  $^g$ ) at  $w = 10 \mu\text{m}$ . (see details in Experimental Section.)

## Supplementary Video captions

**Supplementary Video S1.** Sequential images with the plain electrodes as a function of frequency and voltage.

**Supplementary Video S2.** Sequential images with the fully patterned cross-overlapping electrodes ( $w = 100 \mu\text{m}$ ) as a function of frequency and voltage.

**Supplementary Video S3.** Sequential images with the fully patterned cross-overlapping electrodes ( $w = 80 \mu\text{m}$ ) as a function of frequency and voltage.

**Supplementary Video S4.** Sequential images with the fully patterned cross-overlapping electrodes ( $w = 60 \mu\text{m}$ ) as a function of frequency and voltage.

**Supplementary Video S5.** Sequential images with the fully patterned cross-overlapping electrodes ( $w = 50 \mu\text{m}$ ) as a function of frequency and voltage.

**Supplementary Video S6.** Sequential images with the fully patterned cross-overlapping electrodes ( $w = 40 \mu\text{m}$ ) as a function of frequency and voltage.

**Supplementary Video S7.** Sequential images with the incompletely patterned cross-overlapping electrodes ( $w = 10, 20, \text{ and } 30 \mu\text{m}$ ) as a function of frequency and voltage.

## References

[1] C. A. Schneider, W. S. Rasband, K. W. Eliceiri, *Nat. Methods* **2012**, 9, 671.